Article published online: 2023-05-16

Molecular Layer Deposition (MLD) of a Blocked Mercapto Silane on Precipitated Silica

S. Kim* [a]
J. R. van Ommen[b]
D. La Zara[b]
N. Courtois[c]
J. Davin[c]
C. Recker[c]
J. Schoeffel[c]
A. Blume[a]
A. Talma[a]
W. K. Dierkes* [a,d]

[a] Elastomer Technology and Engineering, University of Twente, 7500AE Enschede, The Netherlands
[b] Department of Chemical Engineering, Delft University of Technology, 2629HZ Delft, The Netherlands
[c] Continental Reifen Deutschland GmbH, 30419 Hannover, Germany
[d] Sustainable Elastomer Systems, University of Twente, 7500AE Enschede, The Netherlands
* s.kim@utwente.nl, w.k.dierkes@utwente.nl

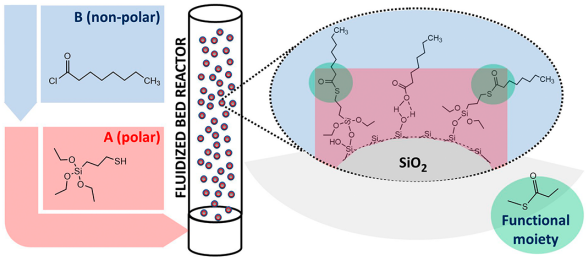

Received: 09.11.2022
Accepted after revision: 30.03.2023
DOI: 10.1055/s-0043-1761310; Art ID: OM-2022-10-0048-OA

Abstract Chemically modified silica is widely used as a reinforcing filler in elastomers. The modification is generally done in situ while preparing the rubber. However, in order to increase the efficiency and facilitate the mixing process, the silica can be pre-treated by a 2-step molecular layer deposition. The precursors for the modification are 3-mercaptopropyltriethoxysilane (MPTES) and octanoyl chloride (OC) to react with MPTES and form a blocked silane. The precipitated silica nanofiller was successfully treated with MPTES and showed a self-limiting behavior: saturation occurred at 2.7%. Furthermore, DRIFTS (diffuse reflectance infrared Fourier transform spectroscopy) analysis confirmed the successful deposition of MPTES on the silica surface by showing the -SH peak that appeared after the reaction of MPTES and silica. In the second step, OC was introduced to form a thioester on the surface of the MPTES-treated silica, controlling the reactivity of the mercapto group from MPTES by blocking it to prevent a negative influence on the processing behavior of the rubber. Thermogravimetric analysis (TGA), Fourier-transform infrared spectroscopy, and X-ray photoelectron spectroscopy (XPS) analytical results confirmed the deposition of the blocked mercapto silane on the silica. TGA results demonstrated the self-limiting behavior of OC, and DRIFTS and XPS proved the thioester formation. A thioester peak after the 2nd reaction step with OC appeared. At the same time, the disappearance of the -SH signal from the MPTES was observed, indicating the formation of the blocked mercapto silane structure. Transmission electron microscopy results showed that the treated silica has a well-distributed carbon and sulfur deposition after MPTES/OC treatment.

Key words: precipitated silica, surface modification, molecular layer deposition

Introduction

Nanoparticles are widely used for various industrial and scientific applications to achieve a specific performance of materials such as polymers. Among the different types of nanoparticles, silica is commonly used as a filler,[1–5] as a catalyst carrier,[6,7] in water purification,[8,9] and for biological and medical applications.[10] As a filler, the silica surface usually needs to be modified by functional chemical groups to improve application performance. For example, silica in situ modified by silane, silica-silane reacted during the mixing step, is a standard filler system in tire technology, mainly for passenger car tire treads as it reduces fuel consumption.[1] However, it has a few drawbacks: an elaborative mixing process[2] and the generation of harmful byproducts during production.[3] In order to overcome these drawbacks, an alternative modification process, such as pre-treatment before the mixing process, is a promising path. Pre-treated silica eliminates the need for adding a coupling agent during the mixing process and improves the mixing performance.[11–14]

Various surface treatment techniques were considered for preparing surface-treated silica, such as conventional solution modification,[2,3,12,15] plasma polymerization,[9,16–20] and

vapor (gas)-phase modification.[21–24] Among these surface modification methods, gas-phase modification offers inherent advantages, such as the absence of a solvent, versatility concerning particle size and structure,[25] and controllability and scalability.[26] Besides, the gas-phase modification can provide a well-structured and dense modification, better than the conventional solution modification.[27] Molecular layer deposition (MLD) is a method to deposit an organic material on a substrate by using alternating precursors.[28,29] This method offers outstanding control over the amount of deposited material by relying on self-limiting surface reactions. Fluidized beds are effective reactors for functionalizing nanoparticles in a gas phase.[30–32] The particles are fluidized in the reactor: suspended in an upward carrier gas (typically N_2) stream with a velocity at which drag and gravity are in equilibrium. The carrier gas flow will also carry the vaporized precursors for modification while fluidizing the nanoparticles.

For the gas-phase modification of silica in a fluidized bed reactor, some requirements are crucial for the precursors:

1. The precursor changes the silica surface to become more hydrophobic and less polar.
2. The precursor leads to functionality which can react with the polymer during vulcanization.
3. The precursor can be transported out of the bubbler by the carrier gas, i.e., it has a sufficiently high vapor pressure at the processing temperature.

Silanes are suitable candidates for silica treatment since they are commonly used in the tire industry.[33] However, most commercially available silane coupling agents such as TESPD, TESPT, and OTPTES (commercial name NXT), as shown in Table 1, have boiling points higher than 250 °C, which is inappropriate for application in gas-phase modification due to the low vapor pressure and, thus, insufficient precursor input.

The screening of precursors for gas-phase modification has led to 3-mercaptopropyl-triethoxysilane (MPTES) as the material of choice. The boiling temperature of MPTES is 210 °C, a relatively low boiling point compared to the other silanes. It is anticipated that this allows for the generation of a sufficiently high precursor gas flow due to the relatively high vapor pressure. The MPTES structure consists of three ethoxy groups on one side of the molecule for coupling to the silica surface. A mercapto (thiol) moiety is attached to the other side of the molecule, which can react with the rubber matrix. It is well known that the reactivity of mercapto silanes is too high to be controlled adequately for most applications in the rubber industry. Besides, it was reported that isoprene-based polymers, including natural rubber or synthetic isoprene rubber, hamper the reaction between the silica and the polymer.[34]

One way to control the reactivity of the thiol is to introduce a protecting group, a compromise between achieving good processing characteristics while mixing rubber and maintaining a high coupling efficiency. Such a blocked silane is actually in use for the in-situ modification of silica, e.g., a 3-octanoylthio-1 propyltriethoxysilane (OTPTES). It is reported that the use of this silane for modification of silica during the mixing process improves the processing behavior and reduces the reactivity of the sulfur moiety compared to the unblocked MPTES.[35,36] Therefore, we propose to achieve this blocking by following the MTPES deposition by the reaction with octanoyl chloride (OC) to form the protecting group. The envisaged reactions of MPTES and OC are depicted in Scheme 1.

Table 1 Commonly used silane coupling agents

Silane	Chemical name	Chemical structure	Molecular weight (g/mol)	Boiling point (°C)
TESPD	Bis(triethoxysilylpropyl)disulfide	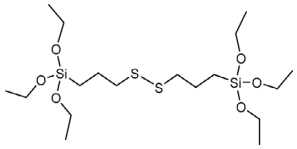	475	> 250
TESPT	Bis(triethoxysilylpropyl)tetrasulfide	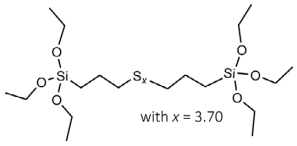	539	> 250
OTPTES	3-Octanoylthio-1-propyltriethoxysilane	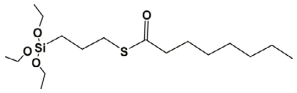	364	> 400

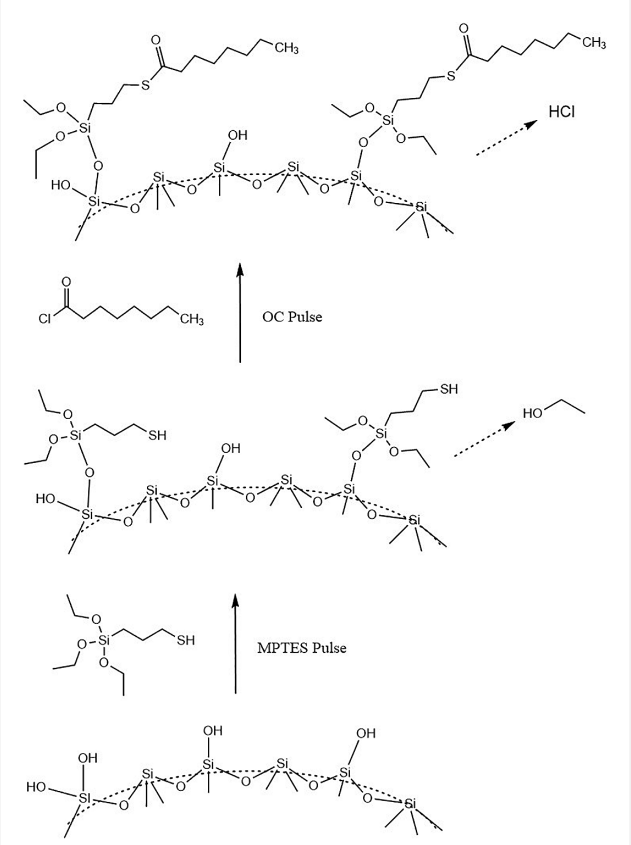

Scheme 1 Mechanisms for the MPTES and OC reactions.

This paper investigates whether MLD of MPTES and OC can modify the surface of silica nanoparticles in a homogenous way, introducing thioester moieties. This is a step towards more effective silica pre-treatment for rubber application.

Results and Discussion

Determination of the Optimal Conditions for MPTES Deposition

After partial or complete MLD treatment, all samples were analyzed by thermogravimetric analysis (TGA) to compare the samples' weight loss, shown in Figure 1. In the first instance, the weight loss increased with increasing pulse time but reached saturation around an MPTES pulse time of 60 minutes. Only minor deviations were found for longer pulses, except for a very long pulse time of 300 minutes, which might have led to disulfide formation or condensation reaction of MPTES.

Figure 2 represents the diffuse reflectance infrared Fourier transform spectroscopy (DRIFTS) spectra of untreated

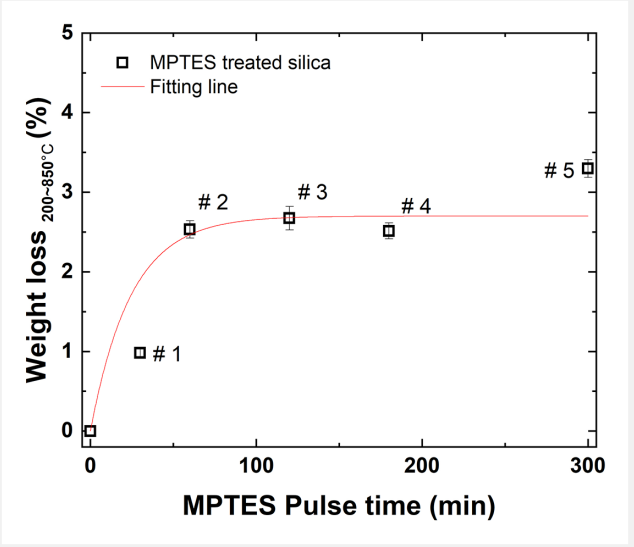

Figure 1 TGA results: weight loss 200 – 850 °C vs. MPTES pulse time. The sample numbers (#) refer to Table 3.

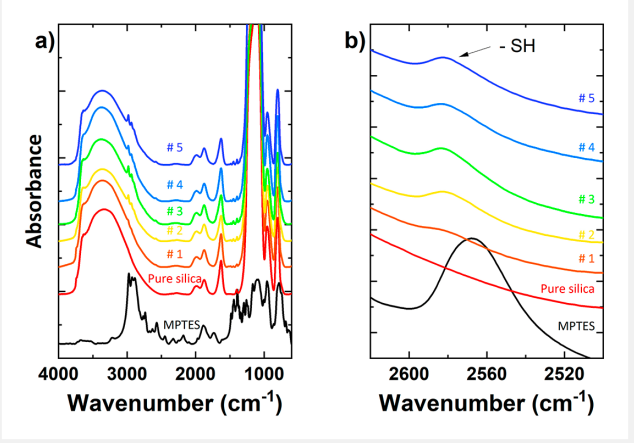

Figure 2 DRIFTS results of MPTES-treated silica: a) full spectrum, b) -SH peak region (2620 – 2500 cm^{-1}).

and MPTES-treated silica after different pulse times. The spectra of MPTES, as such, were also measured to identify the specific peaks of MPTES. MPTES showed the CH band in the range of 3000 – 2800 cm^{-1} and the mercapto group, -SH, at a wave number of 2565 cm^{-1} with a low peak intensity. The MPTES-treated silica showed an increase in the CH band intensity at 3000 – 2800 cm^{-1} with an increase in pulse time; the SH band from MPTES can be followed at ~2580 cm^{-1}.[37,38] DRIFTS and TGA results confirm that MPTES was deposited on the silica surface and actually reacted with the silanol groups on that surface. The combined analyses show that an optimum is reached at a pulse time of > 60 min; a longer pulse does not lead to a further increase in the SH band intensity.

Reaction Conditions for Deposition of OC on the MPTES/Silica Sample

The second reaction introduced OC as a protecting agent for the mercapto group on Sample #3, the MPTES-treated silica sample with optimum coverage. After the treatment with OC, the samples were measured by TGA to determine the weight loss. The weight loss of Sample #3 with only MPTES (2.7%, corresponding to approximately 0.228 µmol of MPTES/g_{silica}) was compared to the weight loss value of the MPTES/OC-treated silica as a reference. After 10 minutes of pulse time, the OC-treated sample showed an increase in weight loss of approximately 0.9% higher than Sample #3. The weight loss value kept increasing with the OC pulse time of up to 30 minutes. Beyond this pulse time, the weight loss value was saturated at around 6.1%, 3.4% higher than Sample #3, corresponding to 0.267 µmol of OC/g_{silica} deposited on the silica. The weight loss of the samples is given in Figure 3.

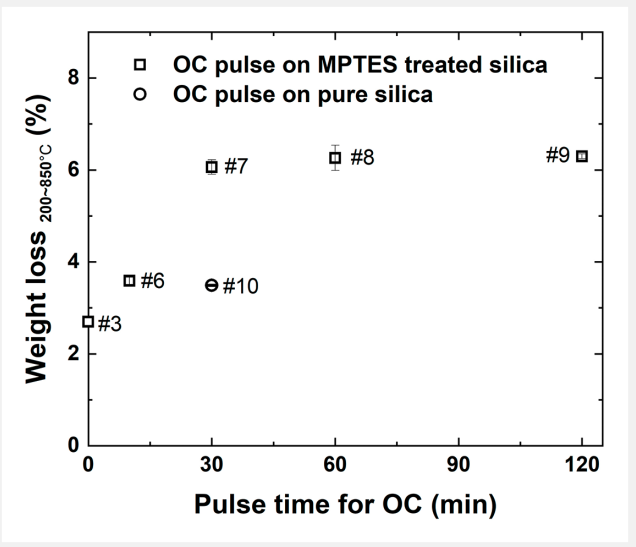

Figure 3 TGA results: weight loss 200 – 850 °C versus pulse time for OC deposition.

The reaction of MPTES bonded to silica with OC is given in Figure 4a. The silica sample reacted only with OC and showed a 3.5% weight loss. OC can react with silanol moieties directly to form an ester group (SiOCO), as shown in Figure 4b, or it can react with water, which was adsorbed on the silica via hydrogen bonding, to form octanoic acid, see Figure 4c.

In Figure 5, Fourier-transform infrared (FTIR) spectra of the modified silica nanoparticles confirm the chemical attachment of OC to the MPTES-silanized silica surface. The full spectra of all studied samples are shown in Figure 5a, including the untreated silica as a reference. The treated samples showed an increase of the C–H band intensity at

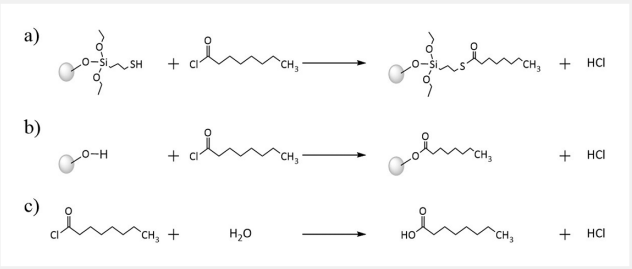

Figure 4 Possible reaction mechanisms between silica and OC.

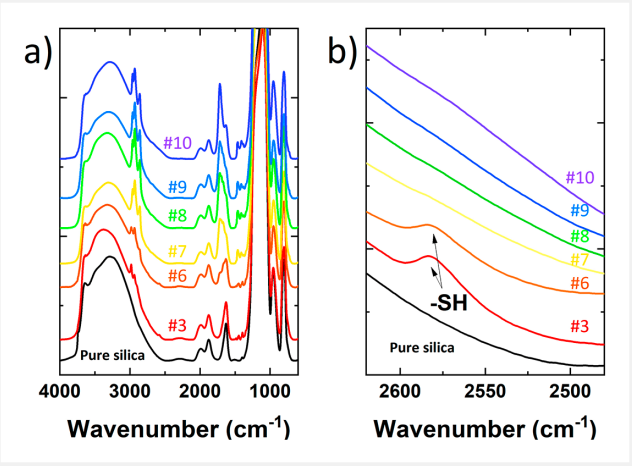

Figure 5 DRIFTS spectra of the untreated and treated silica samples: a) full spectra; b) blow-up of the region between 2650 and 2500 cm^{-1} for the SH group.

3000 – 2800 cm^{-1}, indicating the successful treatment of the silica surface with OC. In Figure 5b, the band at 2580 cm^{-1} corresponding to the S–H bond, which appeared after the reaction of silica with MPTES, disappeared again during the reaction with OC for a longer pulse time than 30 min, which indicates the reaction of the -SH groups from MPTES with OC to form the thioester. The chlorine atom reacts with the hydrogen from the -SH group to form hydrogen chloride.

In Figure 6, the FTIR spectra of the precursors are given. First, the thioester, 3-octanoylthio-1-propyltriethoxysilane, formed by the reaction between MPTES and OC,[39] is detected by the thioester band at ~1690 cm^{-1}. Next, octanoic acid, the hydrogenated form of OC,[40] shows a specific band at ~1710 cm^{-1} corresponding to the carboxylic ester instead of the band at ~1800 cm^{-1} for the halide group from OC.

In Figure 7, the deconvoluted DRIFTS results give more detailed evidence of the reaction between MPTES and OC. In the deconvoluted spectra range of 1900 – 1500 cm^{-1}, the silica samples treated by MPTES/OC show the thioester band intensity at ~1680 cm^{-1}.[41] This proves again that the -SH group reacted with OC in the thioesterification reaction. The halide peak showing a band at ~1800 cm^{-1} was not seen

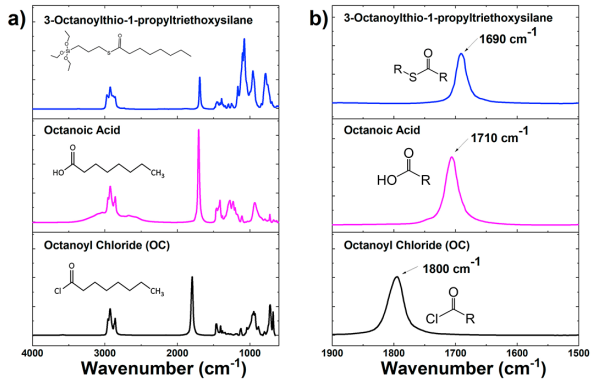

Figure 6 FTIR results of 3-octanoylthio-1-propyltriethoxysilane (reference), octanoic acid, and octanoyl chloride (precursor).

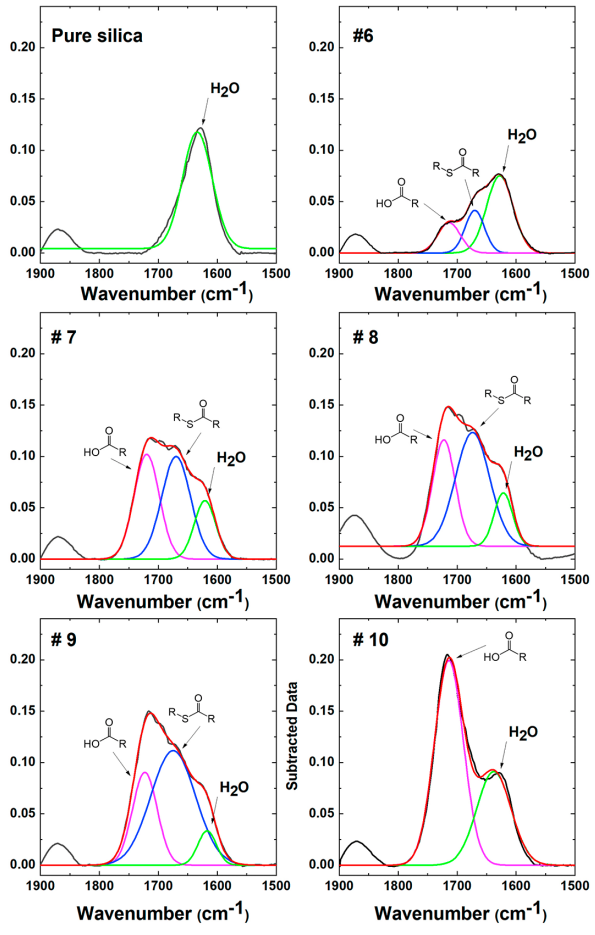

Figure 7 Deconvoluted DRIFTS results of untreated, MPTES/OC, and OC-treated silica in the region between 1500 and 1900 cm^{-1}.

on any of the treated samples, implying that all unreacted OC was removed during purging or converted to octanoic acid by hydrolysis. The latter indicates that the carboxylic peak was detected in all samples with OC treatment. This implies that residual octanoic acid is present, which is not removed during purging due to its high boiling point (> 240 °C). The sample treated with OC only (Sample #10) showed a single carboxylic peak at ~1710 cm^{-1}, indicating that the halide was hydrolyzed to form the acid. No peak indicated the direct reaction between the silanol groups and OC. This reaction does not occur under these circumstances.[42]

The X-ray photoelectron spectroscopy (XPS) spectra of Sample #3 from the first reaction, MPTES treated, and Sample #8 from the second reaction treated with MPTES and OC are shown in Figure 8a, along with the spectra from the untreated silica for comparison. The increment intensity of the peak corresponding to C 1 s in samples #3 and #8 confirms the presence of MPTES and MPTES/OC on the silica surface. The minor C 1 s peak in the reference sample is present due to contaminations or traces of carbon dioxide in the equipment chamber. The S2p scan in Figure 8b showed the S2p doublet at 163.5 and 164.7 eV,[43] respectively, corresponding to the sulfur in the SH group of Sample #3. MPTES/OC-treated silica showed peaks corresponding to the expected divalent sulfur of the thioester at 163.7 and 164.9 eV[41] in the expected 2 : 1 ratio.

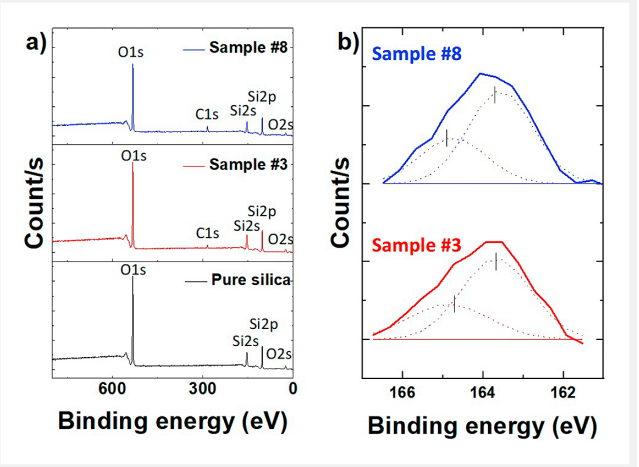

Figure 8 XPS results: a) full spectra of the modified and unmodified silica samples; b) S2p signals of MPTES-treated Sample #3, and MPTES/OC-treated Sample #8.

It is known that commercially available pre-treated silica has the disadvantage that only the external surface of the silica clusters is suitably modified: unmodified silica surfaces are revealed during the mixing process when the clusters are broken into smaller units.[5] Therefore, in order to estimate the modification homogeneity of the MLD process, a crushing test was used to mimic silica cluster breakdown during mixing, followed by XPS analysis. The results are giv-

en in Table 2. The crushed samples #3 and #8 showed comparable surface elemental concentrations with the uncrushed sample, indicating sufficient deposition on the individual nanoparticles.

Table 2 Elemental composition of treated silica (#3 and #8) and crushed samples

Sample		C (%)	O (%)	Si (%)	S (%)
Pure silica		3.1 ± 0.9	68.5 ± 0.5	28.5 ± 0.5	–
#3 (MPTES-treated silica)	Pristine	7.3 ± 0.6	64.0 ± 0.2	28.4 ± 0.5	0.4 ± 0.05
	Crushed	6.3 ± 0.4	65.8 ± 0.5	28.0 ± 0.4	0.3 ± 0.05
	Deviation	***1.0 ± 0.6***	***1.8 ± 0.5***	***0.4 ± 0.6***	***0.1 ± 0.06***
#8 (MPTES/OC-treated silica)	Pristine	12.7 ± 0.5	59.6 ± 0.5	27.1 ± 0.3	0.5 ± 0.05
	Crushed	10.9 ± 0.5	61.9 ± 0.6	27.2 ± 0.2	0.4 ± 0.04
	Deviation	***1.8 ± 0.6***	***2.3 ± 0.7***	***0.1 ± 0.3***	***0.1 ± 0.06***

This implies that the gas-phase reaction relatively homogeneously modifies silica particles. The vaporized MPTES precursor is small, approximately ~1.1 nm, and can penetrate the vacancies of the silica cluster since their estimated size based on a close-packed formation of spherical particles of 20 nm in diameter is 3.1 nm. The gas-phase precursors will react with the isolated silanol or geminal silanol groups on the silica surface. Once MPTES reacts with all reactive silanol moieties, the surface reaction is self-limited, and a condensation reaction between free MPTES and immobilized MPTES on the silica surface barely occurs. As no catalyst was used, the degree of condensation was low.[43]

The morphologies of untreated silica, MPTES (Sample #3), and MPTES/OC (Sample #8)-treated silica samples were visualized by transmission electron microscopy (TEM). Untreated silica has a primary particle size of approximately 20 nm. MPTES- and MPTES/OC-treated silica showed no difference in morphology compared to untreated silica based on several TEM images; an example is shown in Figure 9. These pictures do not show a breakdown of silica clusters into smaller units during the MLD process. Instead, it indicates that the structural properties of the silica are not significantly changed and that the three-dimensional cluster structure is maintained.

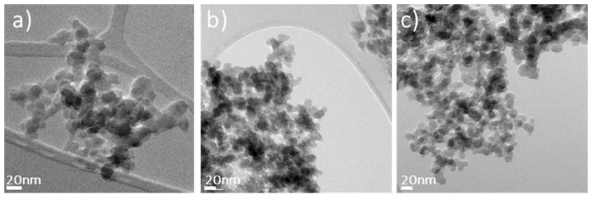

Figure 9 TEM images: a) untreated silica, b) MPTES-treated silica, c) MPTES/OC-treated silica.

Energy-filtering TEM (EFTEM) analysis showed a homogeneous carbon deposition on the silica surface of MPTES/OC-treated silica (#8 MPTES: 120 min/OC: 60 min), as shown in Figure 10, before and after crushing. There is no significant change supporting the previous XPS results.

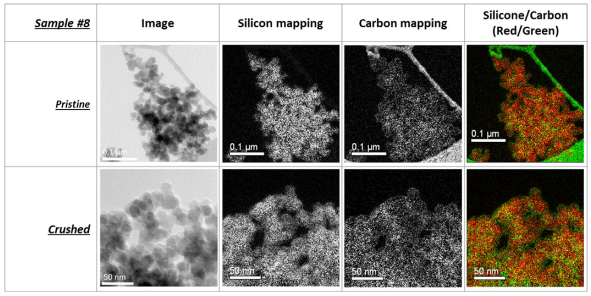

Figure 10 TEM and EFTEM images of the MPTES/OC-treated silica Sample #8 before and after crushing.

Conclusions

Precipitated silica was successfully modified by MLD: MPTES was deposited in the first step, followed by a reaction of OC with the mercapto group of MPTES. TGA, FTIR, and XPS analyses confirmed the successful deposition of both precursors and the formation of the blocked mercapto silane on the silica nanoparticles. The optimal pulse time for MPTES was 120 min, and for OC, 30 min. DRIFTS and XPS proved the thioesterification reaction by the appearance of the SH peak after the first step for the reaction of MPTES and silica, and its disappearance after the second step, the reaction with OC to form the thioester. The treated silica had a well-distributed carbon and sulfur deposition on the outer and inner silica cluster surfaces regardless of the breakage of the silica clusters. This qualifies MLD as a better alternative to the conventional pre-treatment in solution.

Experimental Section

Precursors and Other Materials for MLD

Highly dispersible silica with a specific surface area measured by cetyl trimethyl-ammonium bromide (CTAB) adsorption of 177 m^2/g (ULTRASIL® 7005, Evonik AG, Germany) was used as a substrate for surface treatment. MPTES (purity 98.5%, Sigma Aldrich) was selected as a precursor for the first reaction step for the MLD treatment of the silica samples. The molecular weight of MPTES is 238.4 g/mol, and the boiling temperature is 210 °C with < 2 mbar of vapor pressure at room temperature. As a blocking agent, OC (purity 99%, Sigma Aldrich) was selected as a second precursor.

The molecular weight of OC is 162.7 g/mol, and the boiling temperature is 195 °C, generating a vapor pressure of 0.8 mbar at 20 °C.

Preparation of MLD-Treated Silica in a Fluidized Bed Reactor

MLD was carried out in a reactor consisting of a vertical glass column (50 cm high and 8 cm in diameter) placed on a double-motor vibration table (Paja PTL 40/40 – 24, Netherlands) to assist the fluidization of the silica nanopowder. Two stainless steel distributor plates with a pore size of 37 µm were placed at the bottom and top of the column to obtain a homogeneous distribution of the gas inside the column and prevent particles from leaving the reactor. MPTES was kept in a stainless steel bubbler and heated to 110 °C to increase the vapor pressure. In addition, a second stainless-steel bubbler was added to the setup containing OC, which was also heated up to 110 °C for the sufficiently high vapor pressure of OC. Both vaporized precursors were carried into the reactor by a nitrogen flow (99.999 v/v%) of 2 l/min passing through the bubblers. The lines were heated and kept at 130 °C to prevent condensation and under-delivery of gaseous precursors. The detailed fluidized setup is depicted in Figure 11.

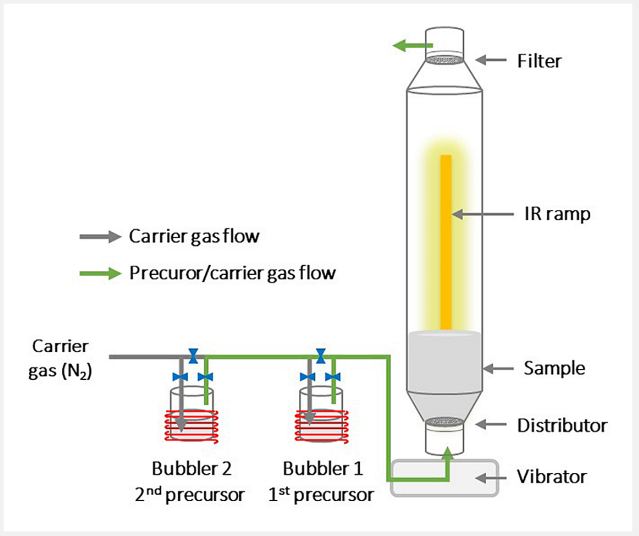

Figure 11 Fluidized bed reactor setup for silica treatment.

Processing Conditions for MLD Treatment of Silica

100 g of precipitated silica was placed in the column. The deposition started with an MPTES pulse followed by an OC pulse through the fluidized bed, with nitrogen purging between the precursor pulses and at the end of the treatment. In addition, silica samples with only MPTES treatment and only OC treatment were prepared for comparison. Optimum pulse times were determined in order to reach surface saturation. The settings for these experiments are given in Table 3.

Table 3 Reaction conditions for MPTES and OC deposition on silica nanoparticles

Sample No.	t_{MPTES} pulse (min)	t_{N2} pulsing (min)	t_{OC} pulse (min)	t_{N2} purging (min)	$T_{bubbler}$ (°C)	$T_{reactor}$ (°C)
1	30	30	–	–	110	200
2	60	30	–	–	110	200
3	120	30	–	–	110	200
4	180	30	–	–	110	200
5	300	30	–	–	110	200
6	120	30	10	30	110	200
7	120	30	30	30	110	200
8	120	30	60	30	110	200
9	120	30	120	30	110	200
10	–	–	30	30	110	200

Characterization of MLD-Treated Silica

TGA (5500, TA Instruments) was used to determine the degree of deposition. It was measured from 30 °C to 850 °C with 20 °C/min ramping rate in an air atmosphere. The TGA weight loss curves were normalized at 200 °C, assuming all physically absorbed water was removed.[44] Therefore, only the weight loss from 200 °C to 850 °C was considered.

FTIR spectra were taken with a Perkin-Elmer Spectrum 100 series equipped with a DRIFTS accessory in the 4000 – 600 cm^{-1} region. Potassium bromide (KBr, FTIR grade, ≥ 99%, Sigma-Aldrich) was used as a reference material for the baseline and sample preparation. KBr was ground and mixed with the silica samples, which were added in a concentration of 10 wt.% to avoid peak intensity saturation during the measurement. Spectra were collected at a nominal resolution of 4 cm^{-1} with 128 sample scans.

Photoelectron spectra were obtained using a Quantera SXM (scanning XPS microprobe) from Physical Electronics. The spectrophotometer was operated under a vacuum of $3 \cdot 10^{-8}$ Torr. A monochromatic Al Kα source (50 W, 148 6 eV) was used for primary excitation at an angle of 45° relative to the sample surface. Survey scans were made to see the gross overall atomic content of the surface layer; they were recorded in the range of 0 to 1200 eV. The measured intensities were in the range of 600 to 12 000 counts s^{-1}. The atomic concentrations were calculated by Equation 1.

$$Cx = \frac{Ix}{Sx} / \sum_{i}^{n} \frac{Ii}{Si}$$

Equation 1

where I_i is the area of a photoelectron peak and S_i is the relative sensitivity factor of the peak. C_x is the fraction of element x, I_x is the peak area of element x, S_x is the relative sensitivity parameter, Σ is the sum of all elements, and n is the number of elements.

TEM and EFTEM were performed in a Philips 300ST-FEG TEM at an acceleration voltage of 300 kV. For the measurements, 0.1 g of silica was dispersed in ethanol by ultrasonication to prepare a suspension. Then a droplet (0.2 µL) of this suspension was put on a Holey carbon film on a TEM grid, and ethanol was evaporated. A GATAN Ultrascan 1000 (2 k × 2 k CCD) camera was used for imaging.

In order to estimate the modification homogeneity within the silica clusters by mimicking the breakdown in the mixer, 1 g of treated silica was ground manually with an agate pestle and mortar until the treated silica clusters turned into a fine powder. XPS and TEM were used to characterize the samples in order to compare the surface coverage of the MLD-treated silica sample before and after crushing.

Funding Information

This project has received funding from M2I under the name of Nanostructured self-assembled functional materials (NANOFUN) and the grant agreement No. C16029.

Acknowledgment

We thank Evonik Industries for providing the silica.

Supporting Information

Supporting Information for this article is available online at https://doi.org/10.1055/s-0043-1761310.

Conflict of Interest

J.R. van Ommen has a financial interest in Delft IMP. This company was involved in upscaling the MLD process for the modification of silica for pilot-scale tire tests. However, the company is not mentioned in the manuscript, as they were not involved in the MLD process development.

References

(1) Rauline, R. U.S. Patent 5,227,425, **1993**.
(2) Mahtabani, A.; Alimardani, M.; Razzaghi-Kashani, M., *Rubber Chem. Technol.* **2017,** *90*, 508.
(3) Alimardani, M.; Razzaghi-Kashani, M.; Karimi, M.; Mahtabani, A. *Rubber Chem. Technol.* **2016,** *89*, 292.
(4) Sarkawi S. S.; Dierkes, W. K.; Noordermeer, J. W. M., *Rubber Chem. Technol.* **2015**, *88*, 359.
(5) Bernal-Ortega, P. M.; Anyszka, R.; Morishita, Y.; di Ronza, R.; Blume, A. *Polymers* **2021**, *13*, 281.
(6) Pullukat, T. J.; Hoff, R.E. *Catal. Rev. Sci. Eng.* **1999**, *41*, 389.
(7) Dorling, T.A.; Eastlake, M. J.; Moss, R. L. *J. Catal.* **1969**, *14*, 23.
(8) Yin, J.; Kim, E.-S.; Yang, J.; Deng, B. *J. Membr. Sci.* **2012**, *238,* 423.
(9) Akhavan, B.; Jarvis, K.; Majewski, P. *ACS Appl. Mater. Interfaces* **2015**, *7*, 4265.
(10) Bitar, A.; Ahmad, N. M.; Fessi, H.; Elaissari, A. *Drug Discovery Today* **2012**, *17*, 1147.
(11) Zhang, C.; Tang, Z.; Guo, B.; Zhang, L. *Compos. Sci. Technol.* **2018**, *156*, 70.
(12) Zaborski, M.; Kosmalska, A.; Gulinski, J. *KGK Kautsch. Gummi Kunstst.* **2005**, *58*, 354.
(13) Ou, Y.-C.; Yu, Z.-Z.; Vidal, A.; Donnet, J. B. *Rubber Chem. Technol.* **1994**, *67*, 834.
(14) Ansarifar, A.; Wang, L.; Ellis, R. J.; Kirtley, S.P. *Rubber Chem. Technol.* **2006**, *79*, 39.
(15) Kapgate, B. P.; Das, C.; Basu, D.; Das, A.; Heinrich, G. *J. Elastomers Plast.* **2015**, *47*, 248.
(16) Arpagaus, C.; Oberbossel, G.; Rudolf von Rohr, P. *Plasma Processes Polym.* **2018**, *15*, 1800133.
(17) He, X.; Rytöluoto, I.; Anyszka, R.; Mahtabani, A.; Saarimäki, E.; Lahti, K.; Paajanen, M.; Dierkes, W.; Blume, A. *Polymers* **2019**, *11*, 1957.
(18) Nah, C.; Huh, M.-Y.; Rhee, J. M.; Yoon, T.-H. *Polym. Int.* **2002**, *51*, 510.
(19) Tiwari, M.; Noordermeer, J. W. M.; Dierkes, W. K.; van Ooij, W. J. *Rubber Chem. Technol.* **2008**, *81*, 276.
(20) Dierkes, W. K.; Tiwari, M.; Datta, R. N.; Talma, A. G.; Noordermeer, J. W. M.; van Ooij, W. J. *Rubber Chem. Technol.* **2010**, *83*, 404.
(21) Mahtabani, A.; la Zara, D.; Anyszka, R.; He, X.; Paajanen, M.; van Ommen, J. R.; Dierkes, W. K.; Blume, A. *Langmuir* **2021**, *37*, 4481.
(22) Fiorilli, S.; Rivolo, P.; Descrovi, E.; Ricciardi, C.; Pasquardini, L.; Lunelli, L.; Vanzetti, L.; Pederzolli, C.; Onida, B.; Garrone, E. *J. Colloid Interface Sci.* **2008**, *321*, 235.
(23) Zhang, F.; Sautter, K.; Larsen, A. M.; Findley, D. A.; Davis, R. C.; Samha, H.; Linford, M. R. *Langmuir* **2010**, *26*, 14648.
(24) Beetstra, R.; Lafont, U.; Nijenhuis, J.; Kelder, E. M.; van Ommen, J. R. *Chem. Vap. Deposition* **2009**, *15*, 227.
(25) van Ommen, J. R.; Valverde, J. M.; Pfeffer, R. *J. Nanopart. Res.* **2012**, *14*, 737.
(26) Van Bui, H.; Grillo, F.; van Ommen, J. R. *Chem. Commun.* **2014**, *53*, 45.
(27) Duchet, J.; Chabert, B.; Chapel, J. P.; Gerard, J. F.; Chovelon, J. M.; Jaffrezic-Renault, N. *Langmuir* **1997**, *13,* 2271.
(28) Yoshimura, T.; Tatsuura, S.; Sotoyama, W. *Appl. Phys. Lett.* **1991**, *59,* 482.
(29) Sundberg, P.; Karppinen, M. *Beilstein J. Nanotechnol.* **2014**, *5*, 1104.
(30) Wank, J. R.; George, S. M.; Weimer, A.W · *J. Am. Ceram. Soc.* **2004**, *87*, 762.

(31) Vasudevan, S.A.; Xu, Y.; Karwal, S.; van Ostaay, H. G.; Meesters, G. M.; Talebi, M.; Sudhölter, E. J.; van Ommen, J.R. *Chem. Commun.* **2015**, *51* 12540.
(32) Van Ommen, J. R.; Goulas, A. *Mater. Today Chem.* **2019**, *14*, 100183.
(33) Wolff, S. *Tire Sci. Technol.* **1987**, *15*, 276.
(34) Sato, M. PhD thesis, University of Twente, The Netherlands, **2018**.
(35) Sengloyluan, K.; Sahakaro, K.; Dierkes, W. K.; Noordermeer, J. W. M. *KGK Kautsch. Gummi Kunstst*. **2016**, *69*, 44.
(36) Ko, J. Y.; Prakashan, K.; Kim, J. K. *J. Elastomers Plast.* **2012**, *44*, 549.
(37) Blume, A.; El-Roz, M.; Thibault-Starzyk, F. 11th Rubber Fall Colloquium. Kautschuk Herbst Kolloqium, Hannover, Germany, **2014**.
(38) Wu, J.; Ling, L.; Xie, J.; Ma, G.; Wang, B. *Chem. Phys. Lett.* **2014**, *591*, 227.
(39) Seeboth, N.; Longchambon, K.; Belin, L.; Silva, C. A. D. U.S. Patent 8,957,155, **2015**.
(40) Sonntag, N. O. *Chem. Rev.* **1953**, *52*, 237.
(41) Aped, I.; Mazuz, Y.; Sukenik, C. N. *Beilstein J. Nanotechnol.* **2012**, *3*, 213.
(42) Launer, P. J. *Silicon Compounds: Register and Review.* Anderson, R.; Arkles, B. C.; Larson, G. L., Petrarch Systems: Bristrol, **1987**, 47.
(43) Ben Haddada, M.; Blanchard, J.; Casale, S.; Krafft, J.-M.; Vallée, A.; Méthivier, C.; Boujday, S. *Gold Bull.* **2013**, *46*, 335.
(44) Ngeow, Y. W.; Chapman, A. V.; Heng, J. Y.; Williams, D. R.; Mathys, S.; Hull, C. D. *Rubber Chem. Technol.* **2019**, *92*, 237.